

# Catalytic Hydroprocessing of Furfural to Cyclopentanol Over Ni/CNTs Catalysts: Model Reaction for Upgrading of Bio-oil

Minghao Zhou · Hongyan Zhu · Lei Niu ·  
Guomin Xiao · Rui Xiao

Received: 30 August 2013 / Accepted: 18 October 2013 / Published online: 1 November 2013  
© Springer Science+Business Media New York 2013

**Abstract** A series of nickel-based catalysts with HNO<sub>3</sub>-pretreated CNTs as support (x% Ni/CNTs, x represents the Ni loading amount) were synthesized using impregnation method, which were successfully applied for the upgrading of model compound (furfural) in bio-oil. Effects of nickel loading amount, reaction temperature, reaction time and hydrogen pressure on conversion of furfural as well as selectivity for cyclopentanol were investigated systematically. The conversion of furfural over 30 wt% Ni/CNTs was up to 96.5 % with a yield of 83.6 % toward cyclopentanol, when the reaction was carried out at 140 °C with a initial H<sub>2</sub> pressure of 5.0 MPa. The features of the Ni/CNTs catalysts were investigated via XRD, XPS, TEM.

**Keywords** Ni/CNTs · Furfural · Hydrogenation · Cyclopentanol

## 1 Introduction

Recently the development of new catalytic processes for preparation of bio-fuel and chemicals using renewable materials has been attracting much attention, due to the rapid consumption of fossil resource [1–3]. Bio-oil is an attractive bio-fuel considering the development of renewable energy sources [1]. As bio-oil contains many kinds of

oxygenated compounds (such as aldehydes, ketones, acids and so on), making it inappropriate as a transportation fuel. So, the quality of bio-oil should be improved by partial or total elimination of the oxygenated functionalities [1, 3]. Mild hydrogenation is one of the promising routes for the upgrading of bio-oil, which could eliminate the most reactive oxygenated groups. Crocker et al. [4] investigated the upgrading of a model bio-oil containing 4 wt% furfural (FFR) over Pt catalysts, which was confirmed to be suitable for the upgrading of bio-oil. And it's reasonable to choose FFR for initial screening, while leaving the investigation of other bio-oil components (such as guaiacol, acetol, etc.) the subject of further research.

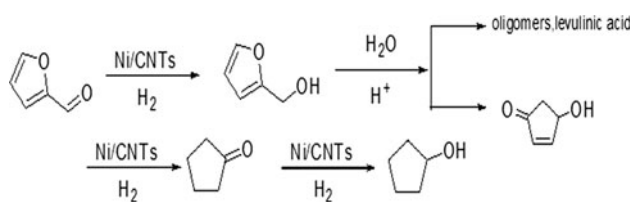
FFR is an important starting material, which can be hydrogenated to prepare furfuryl alcohol, methyl FFR and even longer carbon chain compounds [5, 6], catalyzed by Cu–Cr, nickel based catalysts or noble metal catalysts [1, 7–9]. And cyclopentanol, mainly prepared by catalytic vapor-phase cyclization of 1,6-hexanediol [10] or by liquid phase oxidation of cyclopentene [11], is widely applied for preparation of fungicides, fragrance chemicals. To the best of our knowledge, there has been no report demonstrating the direct hydrogenation of FFR to prepare cyclopentanol using non-noble metal catalysts with satisfactory conversion and selectivity.

Nickel-based catalysts are widely used in hydrogenation, hydrodesulfurization and steam reforming [12, 13]. Although Ni-based catalysts are of lower catalytic activity than noble metals (e.g. Pt, Ru, Rh) [14–16], which are not common in applications for high cost. So it is of significant importance to evaluate nickel-based catalysts with high activity.

Carbon nanotubes (CNTs) was confirmed to be suitable support [17–20], owing to its intrinsic properties such as chemical inertness, thermal stability [21–23]. It was

M. Zhou · H. Zhu · L. Niu · G. Xiao (✉)  
School of Chemistry and Chemical Engineering, Southeast University, Nanjing 211189, People's Republic of China  
e-mail: xiaogmseu@gmail.com; xiaogm@seu.edu.cn

R. Xiao  
Key Laboratory of Energy Thermal Conversion and Control of Ministry of Education, Southeast University, Nanjing, People's Republic of China



**Scheme 1** Possible reaction paths for hydrogenation of furfural in water [24]

reported that ruthenium supported on CNTs exhibited high selectivity toward unsaturated alcohol in the hydrogenation of cinnamaldehyde [17]. However, to develop CNTs-supported non-noble metal catalysts with high catalytic activity remains a challenge. The main aim in this work is to prepare CNTs supported Ni catalysts for the conversion of FFR to cyclopentanol (see Scheme 1). The focus is on the Ni loading amount, reaction time, reaction temperature and hydrogen pressure on conversion of FFR and selectivity for cyclopentanol.

## 2 Experimental

### 2.1 Chemicals

All of the reagents except CNTs are of analytic purity grade, and were purchased from local Sinopharm Chemical Reagent. CNTs was purchased from Chengdu Organic Chemicals Co., LTD (purity >97 %), which was synthesised from natural gas by catalytic cracking method catalyzed by copper-based catalysts.

### 2.2 Catalyst Preparation

Raw CNTs pretreated with concentrated  $\text{HNO}_3$  was selected as support. CNTs was firstly refluxed in 68 wt%  $\text{HNO}_3$  for 12 at 363 K, to increase the concentration of oxygen-containing functional groups on the surface. The mixture was filtered and washed with deionized water, then centrifugated. Each run, the centrifugation process lasted for 5 min under a rotation speed of 9,000 r/min, then washed with water. The process repeated as needed. Finally, the obtained catalysts were dried at 343 K overnight.

Ni/CNTs catalyst was prepared by impregnation method. The support was immersed into an aqueous solution of  $\text{Ni}(\text{NO}_3)_2$  under stirring for 24 h. Then, the obtained solutions were slowly evaporated and the residues were dried at 353 K for 12 h. The obtained solid was calcined at 673 K for 4 h in  $\text{N}_2$ . After grind, it was loaded in a tubular reactor and reduced under  $\text{H}_2$  at 673 K for 4 h. Then it was cooled down and Ni/CNTs catalysts were obtained.

### 2.3 Catalyst Characterization

The prepared Ni/CNTs catalyst was characterized by XRD on a Rigaku D/max-A instrument with a  $\text{Cu K}\alpha$  radiation at 50 kV and 30 mA with a scan speed of  $0.02^\circ/\text{min}$ . The microstructure of the catalyst was examined with transmission electron microscopy (TEM, Tecnai G2 20). The powder sample was dispersed in ethanol and kept in an ultrasonic bath for 2 h, then the sample was deposited onto a carbon-covered Cu supporting grid and dried at  $25^\circ\text{C}$  for TEM analysis. The XPS measurements were performed on an ESCALAB-250 (Thermo-VG Scientific, USA) spectrometer with  $\text{Al K}\alpha$  (1486.6 eV) irradiation source. The elemental concentration and peak's positions were determined with C(1s) peak at 284.6 eV as calibration standard. The Brunauer–Emmett–Teller (BET) surface area were evaluated from the  $\text{N}_2$  adsorption–desorption isotherms using a COULTER SA 3100 analyzer. TG studies were carried out under an air flow rate of 30 ml/min with analyzers by using 10–15 mg sample and a  $20^\circ\text{C}/\text{min}$  temperature increasing. The IR spectroscopy was applied to detect the functional groups on the surface of CNTs.

### 2.4 Catalytic Hydrogenation of Furfural in Water

All the aqueous-phase catalytic hydrogenations of FFR were carried out in a 200 ml stainless autoclave equipped with an electromagnetic driven stirrer. For each run, 95 ml of water, 5 ml of FFR and 1.5 g catalyst were added to the reactor vessel, then the hydrogenation reaction was carried out in a temperature range of 110–150  $^\circ\text{C}$  to evaluate the effect of reaction temperature, for a reaction time of 4–14 h to evaluate the effect of reaction time. Additionally, other influencing factors such as Ni-loading amount and hydrogen pressure were also taken into consideration. After displacing air, the hydrogen pressure was raised to a certain value. Then the reactor was heated to desired temperature and the stirring speed fixed to 600 rpm to eliminate the diffusion effects. Finally, the reactor was quickly cooled down, and the reaction products were separated from the catalysts by centrifugation. The aqueous phase was analyzed using gas chromatography (Ouhua GC 9160) equipped with a SE-54 capillary column ( $30\text{ m} \times 0.32\text{ mm} \times 0.5\ \mu\text{m}$ ). The main products were cyclopentanol and cyclopentanone, and the product yield and selectivity were calculated and defined as follows:

$$X_{\text{FFR}} = \frac{n_{\text{FFR}}^0 - n_{\text{FFR}}}{n_{\text{FFR}}^0} \times 100\%, \quad Y_i = \frac{n_i}{n_{\text{FFR}}^0} \times 100\%,$$

$$S_i = \frac{Y_i}{X_{\text{FFR}}} \times 100\%,$$

where  $i$  represents the product cyclopentanol, cyclopentanone or pentadiol in the reaction;  $n_{\text{FFR}}^0$  and  $n_{\text{FFR}}$  depict the

amounts of FFR before and after reaction, respectively, in mol; and  $n_i$  is the amount of product  $i$ , in mol.

### 3 Results and Discussion

#### 3.1 Catalyst Characterization

##### 3.1.1 Acid Treatment of Raw CNTs

CNTs is a kind of hydrophobic support, which was reported to be difficult to adsorb metal on its surface [25]. Concentrated acids can be used to introduce functional groups (e.g. C=O, COOH and OH) on the surfaces of CNTs [26]. Therefore, CNTs pre-treated with concentrated nitric acids can help to effectively support active metals. The acid treatment cannot only make CNTs form functional groups but can also remove impurities on the surface of CNTs; the results can be analyzed by TGA. From TGA analysis in Fig. 1a, we found that the commercial CNTs contains the impurities about 2.5–3.5 wt%, and acid treatment could help to remove the impurities in the commercial CNTs (see Fig. 1a). The nature of the surface functional groups was investigated by IR spectroscopy, as shown in Fig. 1b. The peak at 1,425/cm was connected with the O–H bending deformation in carboxylic acids. Higher peaks at 1,690 and 3,390/cm were connected with C=O and OH functional groups respectively, which confirmed the presence of C=O and OH functional groups in the acid-treated CNTs. In comparison of the IR results of raw CNTs and acid treated CNTs, it can be found that acid treated CNTs contains relatively large amount of C=O, COOH or OH functional groups, which would help to adsorb active metal on the surface.

#### 3.1.2 Chemical and Physical Properties of Ni/CNTs Catalysts

Table 1 shows the fundamental chemical and physical properties for the CNTs-supported Ni catalysts, including the Ni loading contents, BET surface area and averaged Ni size. The BET surface areas for the Ni/CNTs catalysts range from 107.6 to 145.6 m<sup>2</sup>/g. The averaged crystallite size of Ni/CNTs catalysts (estimated from TEM image) ranges from 8.3 to 20.4 nm, which closely associated with the Ni loading content. The increase of Ni content of the Ni/CNTs catalysts led to the decrease of the BET surface areas [27]. The decreased BET surface areas was mainly caused by the coverage of Ni on the CNTs surface, which can be seen from the TEM test results (Fig. 3). Generally, the increase of Ni content would inevitably lead to the aggregation of particle on the CNTs surface, finally lead to particle growth of Ni. The changes of the catalysts properties would inevitably lead to significant influence on the catalyst activity when increasing the Ni loading content, which were confirmed by the following experiments.

**Table 1** Chemical and physical properties of Ni/CNTs catalysts

Catalyst	Ni content (wt%) <sup>a</sup>	Ni content (wt%) <sup>b</sup>	dTEM (nm) <sup>c</sup>	dXRD (nm) <sup>d</sup>
10 % Ni/CNTs	10.28	145.6	8.3	8.0
20 % Ni/CNTs	19.64	132.4	10.2	9.5
30 % Ni/CNTs	30.36	121.8	13.6	11.7
40 % Ni/CNTs	40.52	107.6	20.4	18.5

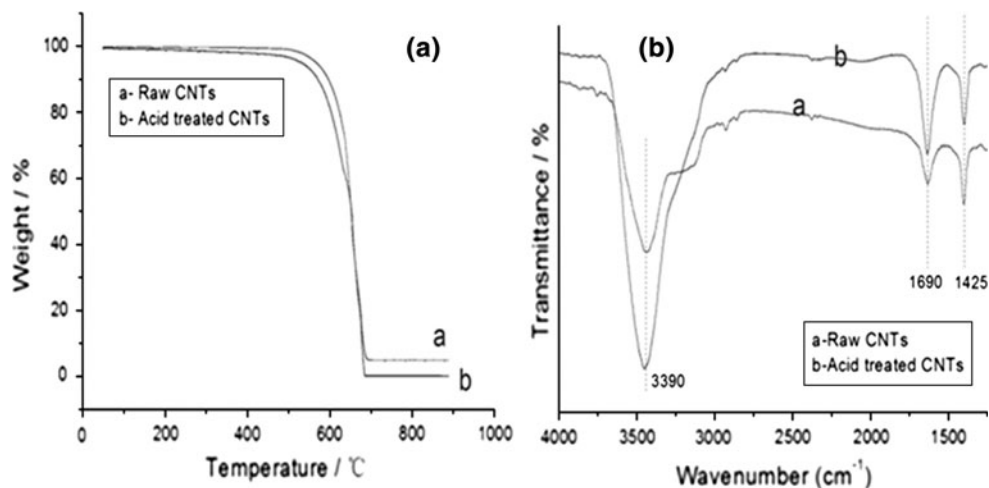
<sup>a</sup> Measured by AAS analysis

<sup>b</sup> Evaluated from N<sub>2</sub> adsorption–desorption isotherms

<sup>c</sup> Measured by TEM analysis

<sup>d</sup> Calculated by Scherrer equation from the peak of XRD

**Fig. 1** TGA spectra and IR spectra of raw CNTs and acid treated CNTs. **a** TGA results, **b** IR results



### 3.1.3 XRD and XPS Characterization

Figure 2a shows the XRD patterns of five different samples, including 10–40 % Ni/CNTs, all reduced by H<sub>2</sub> at 673 K for 4 h, and the used 30 % Ni/CNTs after FFR hydrogenation at 413 K for 10 h. The sharp and symmetric peaks clearly indicate that the samples were well crystallized. The peak at 26.5° could be assigned to the diffraction peaks of the (002) planes of graphite-like tube-wall of the CNTs [17–19]. Besides the CNTs feature, the presence of metallic Ni in the reduced Ni–CNTs catalysts is clearly revealed. As can be seen from the XRD results, only one kind of Ni-based phase was detected for Ni/CNTs catalysts. Peaks at 44.5°, 51.9°, and 76.4° could be assigned to the diffraction of the (111), (200), and (220) planes of metallic

Ni. The used 30 % Ni/CNTs showed sharp and symmetric peaks with little decrease in intensity, which indicated that the catalyst was of good crystal form and stability before or after reaction (see Fig. 2a).

XPS detection was taken to analyze the composition of prepared Ni/CNTs. Absorption peaks were identified for C, O, and Ni. Their mass concentrations were 60.91, 10.71 and 28.38 wt%, respectively. Seen from Fig. 2b, as for the high amount of O, it was caused by the increase of oxygen-containing groups during the treatment of HNO<sub>3</sub>. For another thing, the oxidation of Ni/CNTs catalyst before or during the XPS detection also contributed to the high amount of O. Seen from Fig. 2d, binding energies at 852.9 and 856.3 eV were observed for 30 % Ni/CNTs, corresponding to Ni<sup>0</sup> (2p<sub>3/2</sub>) and Ni<sup>2+</sup> (2p<sub>3/2</sub>), respectively. The

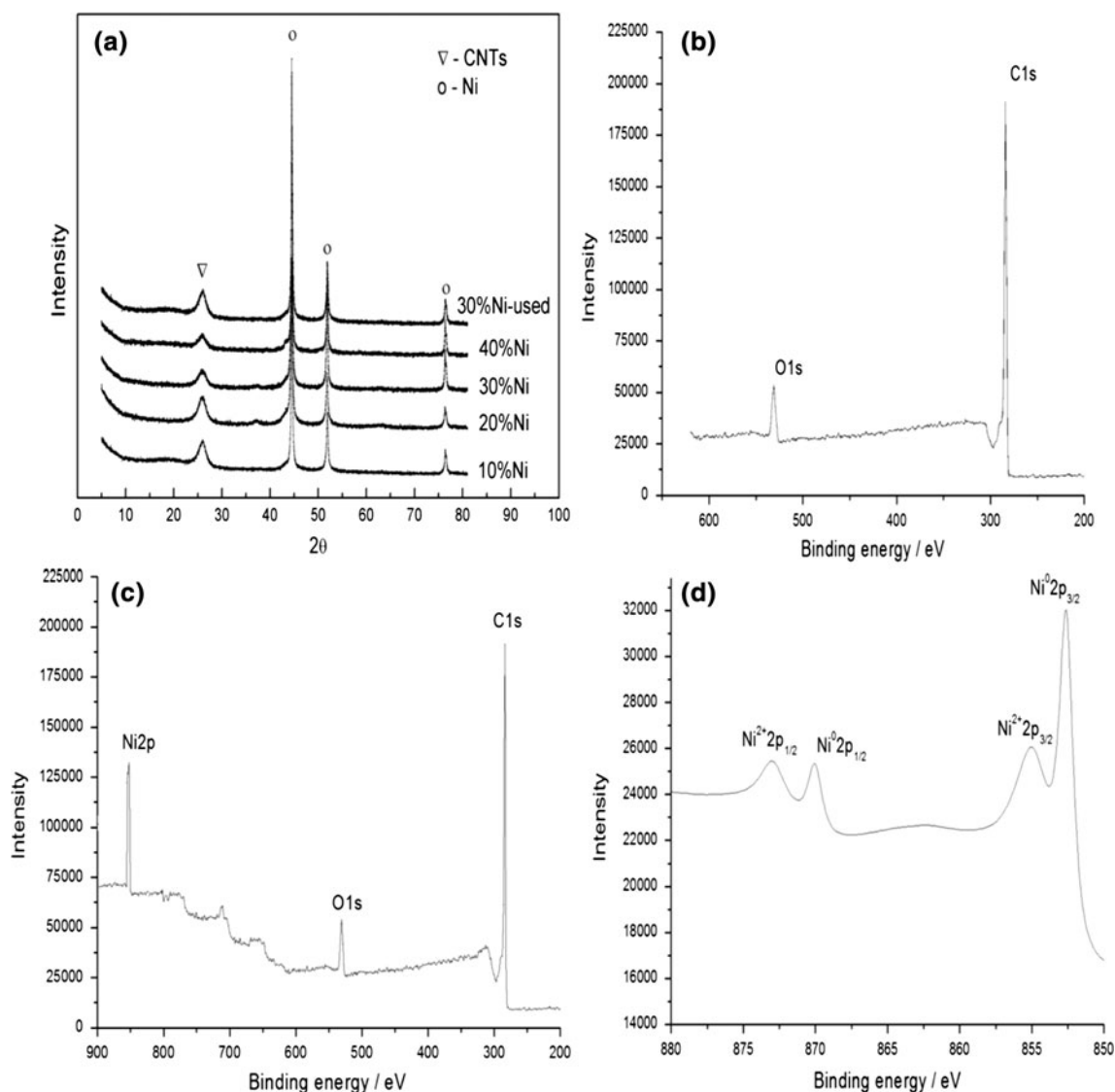
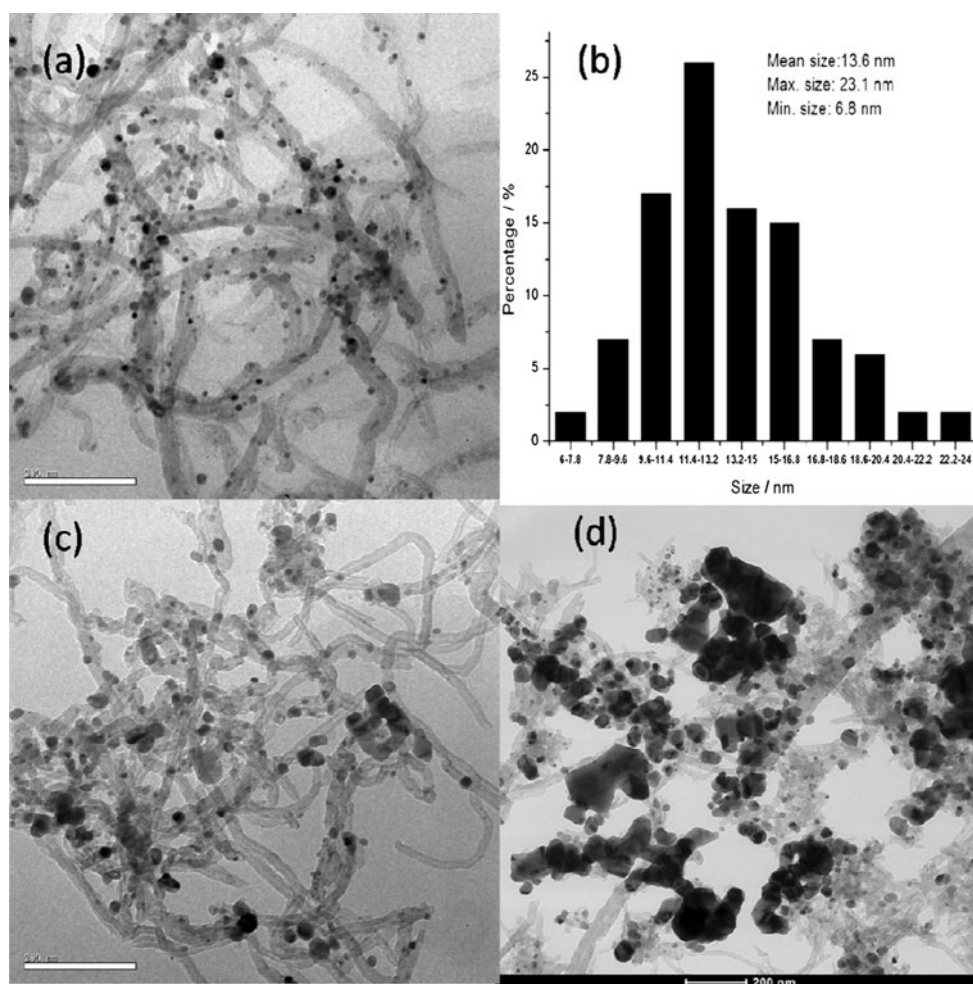


**Fig. 2** a XRD spectra for Ni/CNTs with different Ni content. b XPS pattern of HNO<sub>3</sub>-treated CNTs. c General XPS spectra of 30 % Ni/CNTs. d XPS pattern of Ni2p of 30 % Ni/CNTs

**Fig. 3** TEM images **a** 30 % Ni-CNTs reduced, **b** particle size distribution histogram of 30 % Ni-CNTs reduced, **c** 30 % Ni-CNTs used **d** 40 % Ni-CNTs reduced



binding energies at 872.3 and 874.8 eV correspond to the main lines of Ni<sup>0</sup> (2p<sub>1/2</sub>) and Ni<sup>2+</sup> (2p<sub>1/2</sub>) [27]. It can be found that partial of metallic Ni was oxidised before or during XPS detection, which contributed to the understanding of the high amount of O element.

### 3.1.4 TEM Characterization

As can be seen in Fig. 3, most of Ni particles display outside the CNTs. Thus, the Ni particle size and its distribution mainly depend on loading content. An obvious particle accumulation was observed when Ni-loading increased from 30 to 40 % (see Fig. 3a–d). The histogram of 30 % Ni/CNTs was given in Fig. 3b, in which the mean size was 13.6 nm, smaller than 40 % Ni/CNTs (20.4 nm). TEM result of used 30 % Ni/CNTs (see Fig. 3c) showed little change compared with reduced one, which were in accordance with the XRD result (see Fig. 2). In the following section, it was found smaller Ni particle size with a higher dispersion should be favor to the hydrogenation reaction.

## 3.2 Aqueous-Phase Catalytic Hydrogenation of Furfural

### 3.2.1 Effect of Ni Loading Amount on the Conversion and Product Distribution

As seen in Fig. 4a, the conversion of furfural changes little within all the range of the Ni loading investigated in this work, which suggests there is little effect of the loading amount on the conversion. However, the selectivities toward cyclopentanol (CPOL) and cyclopentanone (CPON) vary greatly, which means the Ni loading has great effect on the product distribution. It can be explained that when adding the Ni amount, the amount of catalytic active site increased for Ni is the most important active site in the reaction. And the varied selectivities were due to the sufficient catalytic active site, which would help to lead to the further hydrogenation to give CPOL with the combined effect of hydrogen in the reaction. Additionally, increase in the loading amount would lead to the decrease in surface area (see Table 1), and cause particle accumulation (see

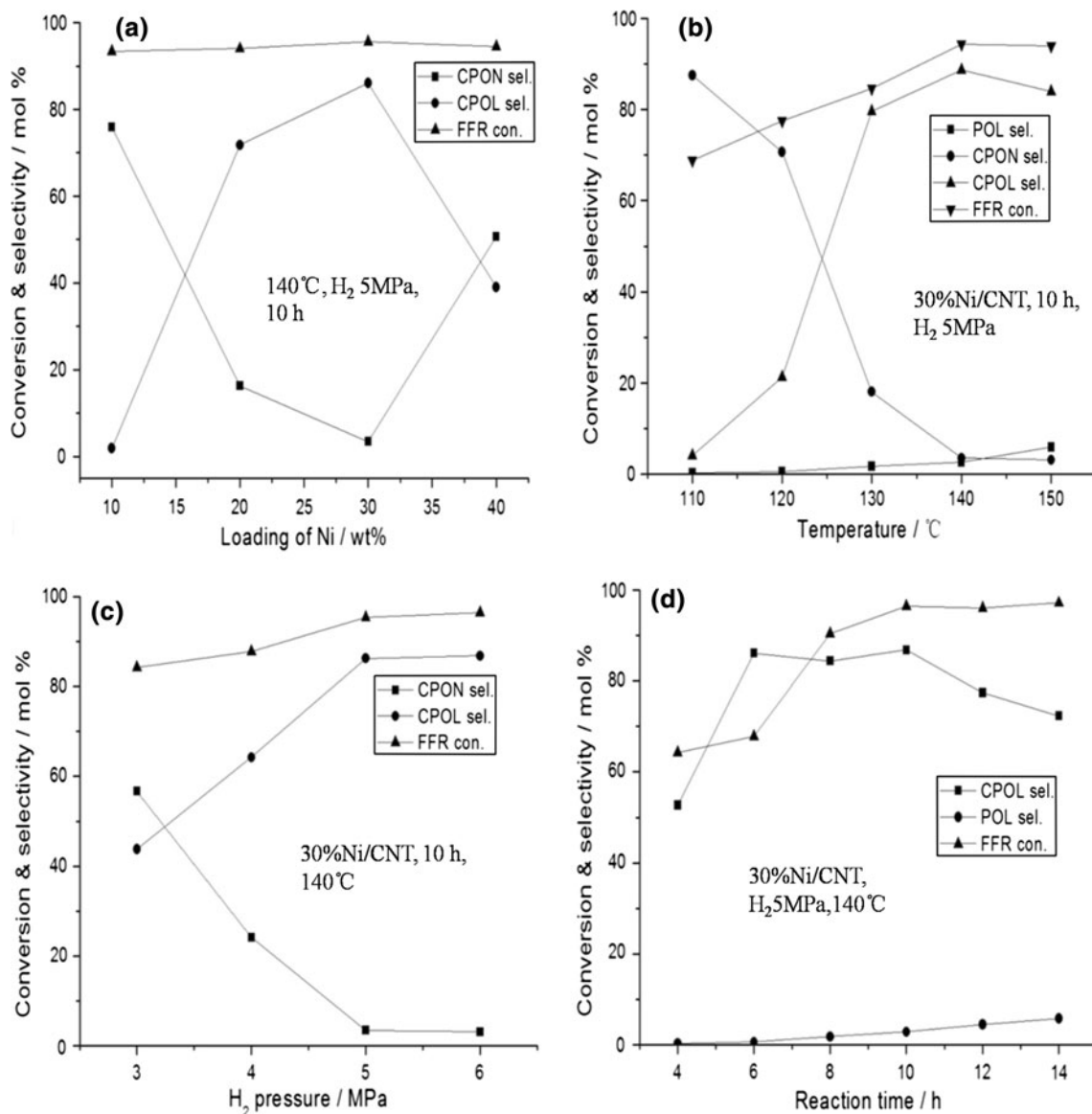


**Fig. 4** Effect of different influencing factors. **a** Ni loading amount, **b** reaction temperature, **c** H<sub>2</sub> pressure, **d** reaction time

Fig. 3), which would influence the catalyst activity [27]. The selectivity toward CPOL reaches the maximum catalyzed by 30 % Ni/CNTs (up to 82.5 %). So, the optimum Ni loading is 30 wt%.

### 3.2.2 Effect of Temperature on the Conversion and Product Distribution

Figure 4b shows the effect of reaction temperature on the conversion of furfural and the reaction selectivity. As seen in Fig. 4b, the conversion of furfural increases from 68.8 to 94.4 % when the temperature increases from 110 to 150 °C and the conversion reaches its maximum at 140 °C (about 96.5 %). Then the conversion decreases a little with the further increase of the temperature. It also can be seen that

the selectivity toward CPOL changes greatly as a result of the change of temperature. The selectivity toward CPOL arrives the maximum of 88.7 % at 140 °C. When the reaction temperature was higher than 140 °C, by-product pentanediol (POL) began to appear as a result of the further conversion of CPOL (Fig. 4b). So, considering the energy consumption and the yield of CPOL, the optimum reaction temperature is 140 °C.

### 3.2.3 Effect of Hydrogen Pressure on the Conversion and Product Distribution

Figure 4c shows the effect of the hydrogen pressure on the conversion of furfural and the reaction selectivities. As seen from Fig. 4c, the conversion increases with the increase of

the hydrogen pressure. When the hydrogen pressure reaches 5 MPa, the conversion is up to 96.5 %. With the further increase of the hydrogen pressure, there is almost no change in the conversion. However, selectivity toward CPOL improved greatly as a result of the increase of hydrogen pressure, which was up to 86.3 % when the hydrogen pressure is 5 MPa. And further increase of the hydrogen pressure shows no obvious improvement in selectivity. The increased CPOL selectivity when increasing hydrogen pressure could be explained by the pushing effect of excess hydrogen on the reaction balance. The reaction balance could also explain why there did not show a continuous increase when continue to increase the hydrogen pressure when exceed 5 MPa. So the optimum hydrogen pressure is 5 MPa.

### 3.2.4 Effect of Reaction Time on the Conversion and Product Distribution

Reaction time is also an important variable that could affect the reaction. In Fig. 4d, the influence of reaction time was presented. As reaction time prolonged, the reaction selectivities toward CPOL increased gradually from 52.7 to 86.9 %. Also, prolonged reaction time would lead to the increase of by-product pentanediol, the yield of which increased from 0.19 to 5.6 %. When the hydrogenation process was carried out for 10 h, the reaction could give both better conversion and selectivity toward wanted CPOL (see Fig. 4d). Thus, 10 h was chosen as the optimal hydrogenation time for prolonged time could not increase the yield dramatically.

### 3.3 Possible Mechanism for the Hydrogenation of Furfural

In this work, a obvious furan ring rearrangement was observed, which could be ascribed to the presence of water as nucleophile and Ni/CNTs. In the first step, the presence of Ni helps weaken the C–O bond, then cause the scission of the C–O bond in the furfural and the formation of a cation intermediate, finally open the ring, as it was reported that furfural could strongly adsorb on metals of Group VIII, especially on Ni based catalysts [28, 29]. Then water contribute to the stabilization and the reaction activity of the intermediate, which is strongly attached on the surface of Ni/CNTs. With the combined impact of Ni/CNTs, water and H<sub>2</sub>, the intermediate finally converted to CPOL. Further studies are still in need for the proposed mechanism.

## 4 Conclusion

Ni/CNTs catalysts were prepared by impregnation method. Furfural could be converted to CPOL with the yield up to

83.6 % catalyzed by 30 wt% Ni/CNTs under 140 °C and the initial H<sub>2</sub> pressure of 5.0 MPa and reaction time for 10 h. And the possible mechanism for the hydrogenation of furfural to prepare CPOL was briefly investigated. The Ni/CNTs composite particles exhibit excellent catalytic performance for the hydrogenation of furfural in water, which was confirmed to be suitable for initial screening of bio-oil upgrading, while leaving the investigation of other bio-oil components the subject of further research.

**Acknowledgments** Authors are grateful for the financial support from the National Hi-tech Research and Development Program of China (863 Program) (2012AA051801) and the National Basic Research Program of China (973 Program) (2010CB732206).

## References

1. Huber GW, Iborra S, Corma A (2006) *Chem Rev* 106:4044
2. Huber GW, Chheda JN, Barrett CJ, Dumesic JA (2005) *Science* 308:1446
3. Petrus L, Noordermeer MA (2006) *Green Chem* 8:861
4. Fisk CA, Morgan T, Ji Y, Crocker M, Crofcheck C, Lewis SA (2009) *Appl Catal A* 358:150
5. Tong X, Ma Y, Li Y (2010) *Appl Catal A* 385:1
6. West RM, Liu ZY, Peter M, Gärtner CA, Dumesic JA (2008) *J Mol Catal A* 296:18
7. Nagaraja BM, Padmasri AH, Seetharamulu P, Hari Prasas Reddy K, David Raju B, Rama Rao KS (2007) *J Mol Catal A* 278:29
8. Huang WP, Li H, Zhu BL, Feng YF, Wang SR, Zhang SM (2007) *Ultrason Sonochem* 14:67
9. Huang F, Li WZ, Lu Q, Zhu XF (2010) *Chem Eng Technol* 33:2082
10. Akashi T, Sato S, Takahashi R, Sodesawa T, Inui K (2003) *Catal Commun* 4:411
11. Kijenski J, Winiarek P, Paryjczak T, Lewicki A, Mikolajska A (2002) *Appl Catal A* 233:171
12. Rajashekharam MV (1997) *J Sci Ind Res* 56:595
13. Reinhoudt HR, Troost R, van Langeveld AD, van Veen JAR, Sie ST, Moulijn JA (2001) *J Catal* 203:509
14. Aupretre F, Descorme C, Duprez D (2002) *Catal Commun* 3:263
15. Domine ME, Iojoiu EE, Davidian T, Guilhaume N, Mirodatos C (2008) *Catal Today* 133–135:565
16. Kugai J, Velu S, Song C (2005) *Catal Lett* 101:255
17. Coqa B, Planeix JM, Brotons V (1998) *Appl Catal A* 173:175
18. Deng WP, Tan XS, Fang WH, Zhang QH, Wang Y (2009) *Catal Lett* 133:167
19. Chambers A, Nemes T, Rodriguez NM, Terry R, Baker K (1998) *J Phys Chem B* 102:2251
20. An GM, Yu P, Mao LQ, Sun ZY, Liu ZM, Miao SD (2007) *Carbon* 45:536
21. Serp P, Corrias M, Kalck P (2003) *Appl Catal A* 253:337
22. Wu G, Chen YS, Xu BQ (2005) *Electrochem Commun* 7:1237
23. Lu CY, Wey MY (2007) *Fuel* 86:1153
24. Piancatelli G, Scettri A, David G, Dauria M (1978) *Tetrahedron* 34:2775
25. Esumi K, Ishiga M, Nakajima A (1996) *Carbon* 34:279
26. Li CH, Yao KF, Liang J (2003) *Carbon* 41:858
27. Hou T, Yuan LX, Ye TQ, Gong L, Tu J, Yamamoto M, Torimoto Y, Li QX (2009) *Int J Hydrogen Energy* 34:9095
28. Bradley MK, Robinson J, Woodruff DP (2010) *Surf Sci* 604:920
29. Pang SH, Medlin JW (2011) *ACS Catal* 1:1272